
About Test-time training for outlier detection

Simon Klütermann *

Department of Computer Science
TU Dortmund University
Germany

simon.kluettermann@cs.tu-dortmund.de

Emmanuel Müller

Department of Computer Science
TU Dortmund University
Germany

emmanuel.mueller@cs.tu-dortmund.de

Abstract

In this paper, we introduce *DOUST*, our method applying test-time training for outlier detection, significantly improving the detection performance. After thoroughly evaluating our algorithm on common benchmark datasets, we discuss a common problem and show that it disappears with a large enough test set. Thus, we conclude that under reasonable conditions, our algorithm can reach almost supervised performance even when no labeled outliers are given.

1 Introduction

Outlier detection is an important subfield of machine learning, with many applications ranging from fault detection[10], fraud identification [21] to science [35, 8]. For these tasks, many algorithms exist, each with their own strengths and faults [16, 41]. Because labeling rare anomalies is an often impossible task, most algorithms work either unsupervised (without any labels) or in a one-class setting (with only normal labels)[37, 23]. Some algorithms [28, 6] are introduced in an unsupervised setting, while other algorithms [42, 3, 9] follow the one-class setting, either explicitly or implicitly.

But in practice, the difference between both is often ignored, as anomalies are rare and most algorithms work with slightly contaminated training data [39]. Therefore, algorithms are trained similarly in both cases. We think that this leaves out important information in the one-class setting, that can be used to improve the performance of outlier algorithms significantly.

An example of this unused information can be seen in Figure 1: Since training and test data are generated by partially different processes, we can measure a difference between their distributions. The higher this difference is, the easier the separation between normal and abnormal data becomes. This paper presents *DOUST*, our method that searches for a data representation explicitly maximizing this difference.

DOUST uses the contaminated test data it is applied to (test-time training [45]), to specialize a simple outlier detector to work better at finding anomalies in the same test data. This approach can be seen as the benefit of knowing the questions of an exam already while studying for it: While the pedagogical use might be questionable, using all available information increases the quality of the answers. Similarly, we reach a drastically superior outlier detection performance that is comparable to supervised classification, even when no labeled outliers are given. We believe that only needing normal samples to reach effective classification performances makes our method applicable to many applications. Examples situations contain provably fault-less historical data[34] or tasks where simulated data exists [33].

*This work was supported by the Lamarr-Institute for ML and AI, the Research Center Trustworthy Data Science and Security, the Federal Ministry of Education and Research of Germany and the German federal state of NRW. The Linux HPC cluster at TU Dortmund University, a project of the German Research Foundation, provided the computing power.

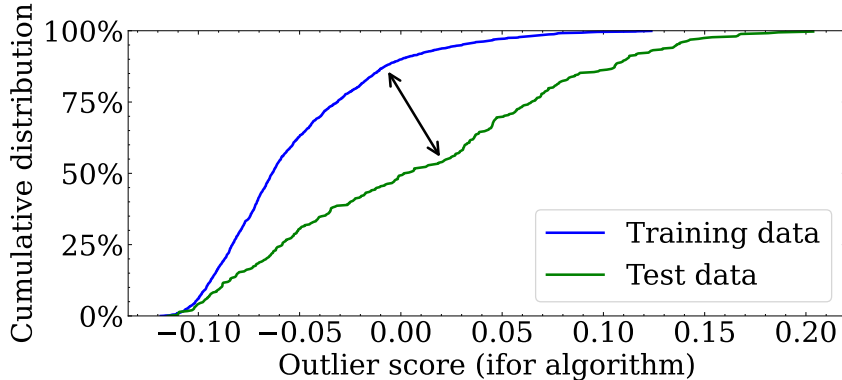


Figure 1: Cumulative distribution of anomaly scores of an isolation forest [28] on cardio data [15]. There is a difference between training data (100% normal) and test data (50% anomalies), which our approach tries to maximize.

After summarizing related work in Section 2, we will explain our method and carefully evaluate it in Section 3 and finish by mitigating a common problem in Section 4.

To increase reproducibility, or code is available at anonymous.4open.science/r/doust-15EE

2 Related Work

2.1 Outlier Detection

Outlier detection is the task of finding samples that "deviate(s) considerably from some concept of normality" [41]. Most of the research in this direction is either done unsupervised, without access to any labels, or as one-class learning when only considering normal samples to train a model [37].

There are many methods [16, 41], that can be separated into shallow classical methods [28, 19, 14, 3], and deep learning methods [44, 32]. Historically, most shallow methods were originally suggested to be trained unsupervised, while deep learning methods employ train test splits, inviting the one-class setting. Still, the methods mentioned are often applied in both situations, as a contamination [39] of the training set usually only slightly decreases their performance. Instead, our method, *DOUST*, explicitly uses the additional information given in the one-class setting to improve the outlier detection performance and can thus only be trained on a clean training set without anomalies.

But, compared to active learning [48] or semi-supervised learning, *DOUST* requires no expensive labeled outliers to be trained.

DOUST is a deep-learning method since this allows us to change the learning behavior through a loss function easily. Additionally, deep learning methods generally are able to learn more complicated separations, allowing us to find even more difficult outliers [41].

Our method bears similarities to DeepSVDD [42] and DEAN [7], as it also tries to learn a constant representation. While similar methods could likely also be applied to different deep learning methods, the direct link between the optimization goal and anomaly score of these methods makes designing effective losses here significantly easier.

2.2 Test time training

Test time training is a relatively new concept in supervised learning [45] [12]. It tries to solve the problem that training data often differs from test data, especially from data used in production environments. For example, a face recognition system might break when everybody suddenly starts to wear face masks. Their approach combines a supervised algorithm, which could not be trained on test data since the test labels are missing, with an unsupervised algorithm that could still be trained

without labels. This can allow them to refine learned hidden features to better match test data, even under a possible distribution shift[27], making it a subsection of unsupervised domain adaption [29].

This approach is not susceptible to overfitting even though test samples are used since no access to the test labels is given.

In supervised test-time training, the major difficulty is that there might be a misalignment between the supervised and the unsupervised optimization goals. But in the one-class setting studied here, we do not need to combine two models, as our training is anyhow independent of supervised labels. Because of this, many older outlier detection papers do not separate between training and test data[6]. And some algorithms[28] even work slightly better when using finding outliers in their training data.

And while we need to optimize our model not only during training time but also during test time, this is no different from how, for example, a k-nearest neighbor outlier detection algorithm [14] searches for outliers: Except for some pretaining to increase the efficiency, most computation time is done during testing, by evaluating the difference between training and test samples.

DOUST extends these ideas to modern deep learning methods, explicitly searching for differences between distributions during test time.

2.3 Positive unlabeled learning

In positive unlabeled (PU) learning, a machine learning method considers both a set with samples from a positive class and a set of unlabeled samples [2]. This is usually studied in supervised learning (For example, a missing medical diagnosis only indicates that a patient could be healthy or sick), but can also be extended to outlier detection. The most common application is semi-supervised learning [43], where an unlabeled set of both normal and abnormal samples and a positive set of a limited number of known anomalies is given. This tends to work better than unsupervised methods [16], but only as long as anomalies are similar to the anomalies used for training.

PU learning can also be used when a set of normal and a set of unlabeled samples are given, even though this is less developed. For example, PU learning can be used similarly to a modern reject option [26], removing outliers from a classification task. Other papers focus on indirect optimizations to improve existing outlier detection methods, like threshold selection [46] or model selection [1]. A more direct method is studied in [49, 36] , by trying to transfer the PU learning task to a usual classification task through an iterative approach, selecting the most anomalous samples from the unlabeled set, and training a supervised algorithm on this set. This has a drawback similar to the semi-supervised approach: Only anomalies similar to these most anomalous samples can be found. Also, the iterative approach can allow singular mistakes in the original assessment of anomalousness to snowball into a misalignment between the type of samples found and the outliers searched for.

In contrast, *DOUST* tries to directly maximize the difference between both sets, making it less susceptible to an initial outlier assessment. Additionally, through the use of test-time training, we do not require our anomalies to generalize, as we search for them directly on the test set we find them directly on the test set. This also means that we do not need to collect additional unlabeled data for our training phase.

3 Outlier refinement with Test time training

Outlier detection is often done in a one-class setting, where only normal data points are known. As shown in Figure 1, this implies that there is a measurable difference between the distribution of data used for training and that used for testing. Our idea is to create a one-dimensional data representation that maximizes the difference between training and test samples, and thus also between normal and abnormal ones (as shown in Appendix D. Exceptions are studied in Section 4). This representation can thus be used as an outlier score, where higher values represent more anomalous samples.

Our method, Deep OUTlier Selection with Test-time training (*DOUST*), contains two training steps. One pertaining step during training time, and one to refine our model on the test data.

After defining a neural network (our specific hyperparameter choices can be found in Appendix A) to transform samples to a one-dimensional representation, we first train it to learn a constant value for

each sample in the training set (following [42, 7]) using the loss function defined in Equation 1.

$$L_0 = \sum_{x \in X_{train}} (f(x) - \frac{1}{2})^2 \quad (1)$$

We use a special activation function (Equation 2) in the last layer of our neural network:

$$S^+(x) = S(x - 1) = \frac{1}{1 + e^{1-x}} \quad (2)$$

This shifted sigmoid fulfills $S^+(x) \in (0, 1)$, simplifying later calculations, but also does not satisfy the trivial solution of $S(0) = \frac{1}{2}$, which would trivialize the loss in Equation 1.

After this first step, removing some of the uncertainty of random initialization, pre-tuning the network for outlier detection, and setting all values close to the middle of possible distribution values, we will add a second step, pulling apart normal from abnormal samples. This second step is part of the evaluation since it requires access to our test data. It allows us to specialize our prediction to the specific outlier detection task. This also means that when evaluating our algorithm on new data, the second training step needs to be repeated to achieve maximum performance.

In the second step, many functions are possible, and we will study these further in Appendix J, but here we study a slightly modified mse loss (Equation 3). This loss desires each training sample representation to be as small and each test sample as high as possible.

$$L = \frac{1}{\|X_{train}\|} \sum_{x \in X_{train}} f(x)^2 + \frac{1}{\|X_{test}\|} \sum_{x \in X_{test}} (1 - f(x))^2 \quad (3)$$

Since many samples from the test set follow the same distribution as those from the training set, this does not actually separate training from test samples but rather separates normal from abnormal ones. To show this, we assume infinitely many samples equally distributed over the training and test set: $\|X_{train}\| = \|X_{normal}\| \rightarrow \infty$. Also, we assume that the training data is sampled from a distribution p_{normal} , while the test data follows $(1 - \nu) \cdot p_{normal} + \nu \cdot p_{abnormal}$ (with the fraction of abnormal data samples in the test set ν). Rewriting Equation 3 with these assumptions, we find:

$$L \propto \int_{\mathcal{R}^d} dx p_{normal}(x) \cdot (f(x)^2 + (1 - \nu) \cdot (1 - f(x))^2) + p_{abnormal} \cdot \nu \cdot (1 - f(x))^2 \quad (4)$$

This loss is minimal, when $f(x) = 1$ for all abnormal samples and $f(x) = \frac{1-\nu}{2-\nu} \leq \frac{1}{2}$ for all normal samples. While practical implementations have further complications, limiting this relation (Limited neural network complexity, sampling uncertainty, contamination, which are partially studied in Appendix F), this relation allows *DOUST* to explicitly optimize finding samples without knowing what they look like.

During implementation, we found that using an ensemble (similar to [7], using 100 submodels) is slightly beneficial (Appendix G.1). But also that feature bagging should not be used (In contrast to [7], see Appendix G.2). These kinds of optimizations were only done once on one unrelated dataset[31], to not taint our shown results (See Appendix H)

3.1 Experimental comparison

This we will now evaluate experimentally. For this, we follow a recent survey paper [16]. We choose the benchmark datasets studied there (even though we restrict ourselves to the 47 datasets they consider classical to limit the computational cost (see Appendix I) and choose the three best algorithms they found as competitors. These are a k-nearest neighbor algorithm[14], an isolation forest [28], and cblof [19] (a cluster-based extension of lof[6]). Additionally, we compare against a supervised random forest algorithm [5]. As the datasets are designed to work well with unsupervised algorithms, we only use the test set of these algorithms for the random forest but employ cross-validation [40] to remove overfitting effects. More details about our competitors can be found in Appendix B.

To evaluate a models performance, we will use the ROC-AUC score, as it is independent of the fraction of anomalies (ν in Equation 4). This is required for some of our analyses (See Appendix C).

3.2 Handling erroneous models

Some training loops fail because of the higher complexity of the models we suggested. And while there are always hyperparameters that could be changed (for example, each task is solved by at least one of the loss functions described in Appendix J), the high number of models we train (Appendix I), makes optimizing specific model impossible. Additionally, this might result in unfair comparisons when comparing differently trained algorithms.

Instead, we ignore these measurements by removing datasets on which not every used algorithm worked. This means that we will use different datasets in each comparison, and numeric results are usually only comparable in each diagram. We will clarify how many datasets could be used for each result, but each result uses at least half of all datasets outside of Appendix J.

Erroneous models usually happen in one of three ways:

1. When a training loop only sometimes fails but also works sometimes, we will ignore this error. This is possible since each performance is the performance of an ensemble with (up to) 100 submodels, but these ensembles usually converge already at 5 – 10 submodels. Thus, combining a few fewer models does not meaningfully affect the results. Solving this would also only decrease the increase of our algorithm.
2. If a training loop does not run successfully at all, we will remove this dataset. This happens only rarely (2 of 47 datasets), but this can still become significant when comparing multiple settings.
3. In Section 4, we will modify our datasets by altering the fraction of anomalies ν . This can result in datasets without anomalies, which will also be removed. Because of this, a maximum of 31 datasets are possible here.

3.3 Experimental results

We summarize our results as a critical difference plot in Figure 2. This critical difference plot compares the performance of each model to each other and marks differences that are not statistically significant (like ifor and cblof). For this, we use a Friedman test [11] to see if there are any significant differences between the methods. Afterward, a Wilcoxon test [47] test determines which of the differences are significant. For this, we consider p-values below $p < 5\%$ (after a Bonferroni-Holm correction [22]) as significant. The corresponding ROC AUC values for each dataset can be found as a table in Appendix K.

Even though our unsupervised competitors are some of the effective algorithms for finding anomalies on these datasets [16], the average rank of our algorithm is significantly better. The change in ROC-AUC is even more significant, with our algorithm performing more than twice as close to a perfect separation of 1 than each unsupervised competitor.

But perfect separation is only rarely possible since datasets are usually imperfect and distributions overlap. A more reasonable limit is the supervised random forest (An algorithm using unlabeled data should perform worse than one with access to labels [37]). Here, our algorithm performs 99% as well as this limit, with only an insignificant difference in our datasets. This is surprising since it effectively means we are able to find outliers almost equally well, whether we have access to labeled outliers or not.

4 Optimization misalignment

For most outlier detection algorithms, the fraction of anomalies in the test set (ν) does not affect the predictions or the results (when using ROC AUC [17] for evaluation). We have already seen in Section 3, that the optimal separation between normal and abnormal data is $\Delta = 1 - \frac{1-\nu}{2-\nu} = \frac{1}{2-\nu}$. This means the fewer anomalies are in the test set, the smaller the separation between normal and abnormal samples. But this difference can often either be ignored (at $\nu = 1\% \rightarrow \Delta \approx 0.503$, while at $\nu = 5\% \rightarrow \Delta \approx 0.513$) or fixed (See Appendix F). Still, Figure 3 shows a clear effect of ν on the

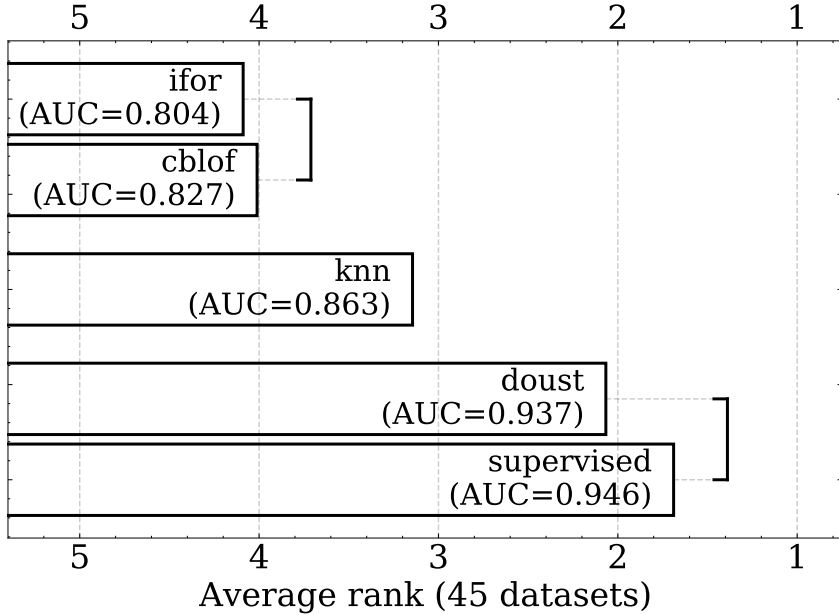


Figure 2: Critical difference plot. We also add the average ROC AUC of each algorithm. As expected, the three unsupervised algorithms perform worse than the supervised ones. But *DOUST* performs almost as well as the supervised random forest (there is no statistically significant difference between their performance at $p = 5\%$).

average performance. Thus, a more devious effect must make our algorithm depend on ν . This effect will be explained and combated in this section.

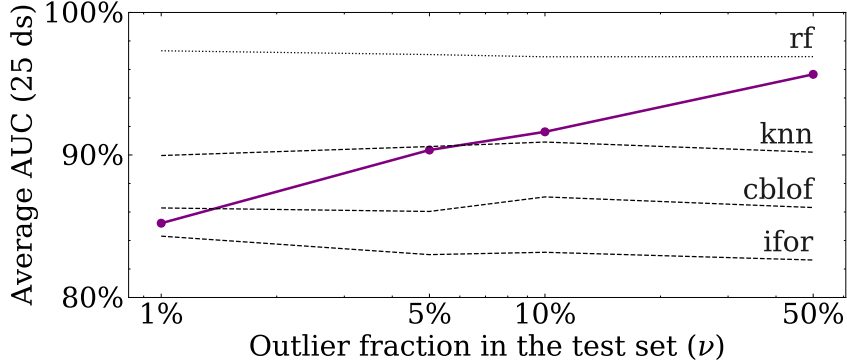


Figure 3: Comparison of the average AUC, of our algorithm (blue), compared to our competitors (black), as a function of the fraction of anomalies in the test set ν . To increase readability, we use a logarithmic x-axis.

Our performance is very competitive for a fraction of $\nu = 50\%$ anomalies in the test set; it becomes more average at single-digit values of ν and seems to drop off further for even lower anomaly fractions. So, to have an algorithm that is also useful in real-world applications (anomalies are rarely as common as $\nu = 50\%$), it is important to understand the effect driving this change.

Looking at Figure 3, it is worth noting that our competitor's performance also changes. This is because we remove outliers from our test set until ν is approximately fulfilled (thus, we also average slightly different outlier fractions and remove datasets with less than 200 outliers). And while the resulting ROC-AUC performance does not change on average, it still fluctuates depending on whether

we remove easy or hard-to-find outliers. Thus, a better interpretation of Figure 3 is that the average AUC drops compared to our competitors.

To explain why this happens, we suggest a thought experiment. Given a normal distribution of samples, we would like to find outliers that do not conform to this distribution. To do this, we can choose one of two thresholds: one right and one left of our data, and we choose the threshold that separates more points. We visualize this thought experiment in Figure 4.

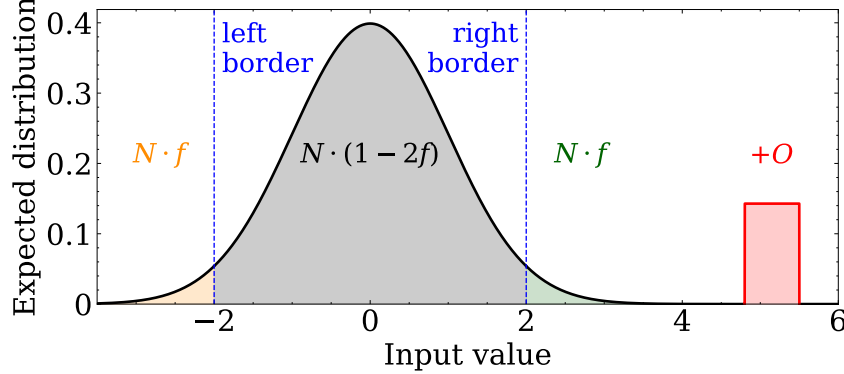


Figure 4: Visualization of our thought experiment. We consider two distributions. One that is normal is shown in grey, and one that is abnormal further away (red). To find this distribution, we consider one of the blue lines as a threshold, depending on which threshold separates more samples.

We want to answer how likely it is that the right side is chosen, and thus the outliers are found. For this, the right side needs to contain more samples than the left one: This will consistently happen when there are enough outliers O , and the outliers are found in close to 100% of cases, but if $O \ll N \cdot f$, then it becomes more likely that random fluctuations dominate the number of samples on both sides and thus the probability drops to 50%. We simulate this behavior in Figure 5.

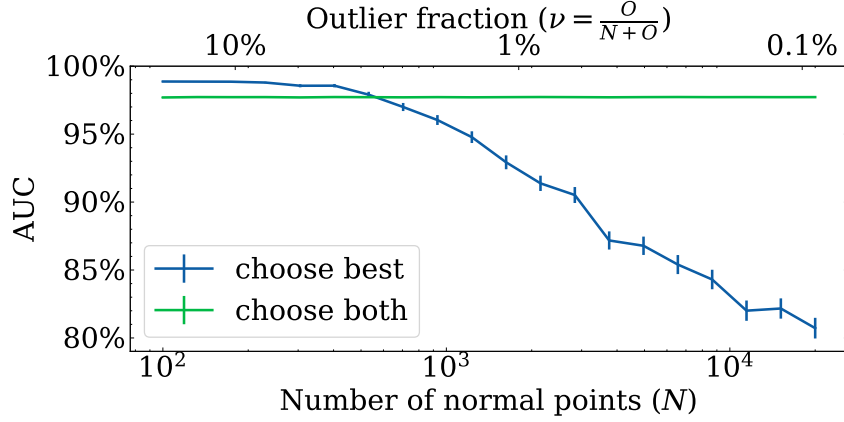


Figure 5: Experimental results of our thought experiment (in blue). When increasing the number of normal samples considered and thus decreasing the outlier fraction ν , the ROC-AUC drops, representing a worse separation. This is because it is less likely that the right threshold will be chosen. For comparison, the green line represents a model that considers both samples outside both thresholds as outliers, similar to a classical unsupervised outlier detector.

At some point, it becomes likely that the random fluctuations of the normal distribution dominate our experiment. Thus, the outliers of the normal samples are more significant than those that we consider anomalous, creating a misalignment. Because there are too few anomalies, these are not captured by our loss, and our algorithm prefers searching for differences between the two normal distributions.

Alternatively, when always considering samples on both sides as anomalous, the performance might be worse for a high ν , but stays constant. Applying this to our original comparison, this can be seen as an algorithm not specified on a specific outlier detection dataset but used to find each type of outlier (like our unsupervised competitors). While the ROC-AUC performance is competitive, consider that this algorithm consistently has twice the number of false positives, resulting in its making more mistakes than the blue line for each ν (See Appendix C.1), limiting the effectiveness of this type of outlier detector.

Mathematically, we can find a region in our thought experiment in which the algorithm searching for the right separation always reaches the right conclusion. Namely, we search for the region in which the uncertainty of the number of normal points is significantly lower than the number of added anomalies. We assume the number of normal points to follow a binomial distribution with mean $N \cdot f$. Using the uncertainty of a binomial distribution $\sqrt{N \cdot f \cdot (1 - f)}$, we can write this condition as:

$$\sqrt{N \cdot f \cdot (1 - f)} \ll O \Leftrightarrow f \cdot (1 - f) \ll O \cdot \frac{O}{N} \quad (5)$$

Here f represents the separation between normal and outlier distribution. The higher the separation, the lower f and the easier it is to fulfill the condition. We usually don't know f , but we can limit it from above, as $f \in (0, 1)$ and thus $f \cdot (1 - f) \leq \frac{1}{4}$.

As expected, Equation 5 becomes harder to fulfill when anomalies are rare (Assuming $O \ll N$, $\frac{O}{N} \approx \nu \rightarrow 0$), but it also becomes easier to fulfill when there are more anomalies ($O \rightarrow \infty$). This implies that for a fixed outlier fraction ν , the more measurements there are, the more likely the separation succeeds.

As a rule of thumb, we require approximately $N \gg \frac{1}{\nu^2}$ samples.

Because of our downsampling strategy, we effectively decrease the performance in Figure 3 twice, as we do not only decrease the fraction of anomalies $\frac{O}{N(+O)}$, but also the total number of anomalies (Also see Appendix E).

This means to test whether this effect generalizes for more than our thought experiment, we have to rely on simulated data. This we do in Figure 6; we apply our method to find anomalies on ten-dimensional simulated data, where normal and abnormal distributions are Gaussian, with $\mu = \vec{0}$, $\vec{1}$ and $\sigma = \vec{1}$ as well as low contamination of $\nu = 1\%$. More details can be found in Appendix A.3.

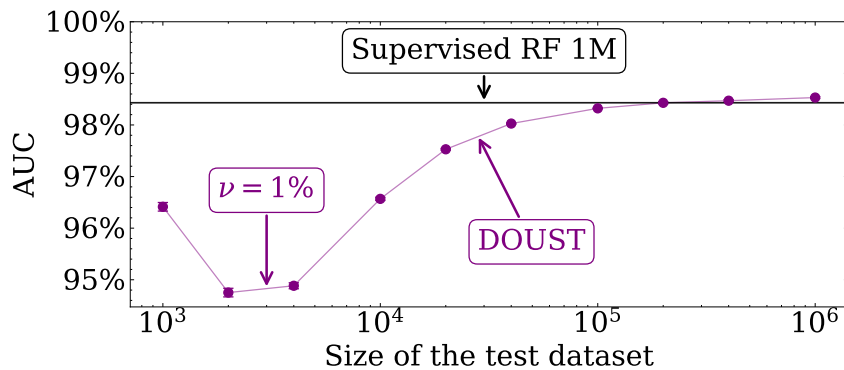


Figure 6: ROC-AUC score of *DOUST* on simulated data with a low contamination of 1%. While for a low number of measurements, the AUC is worse, it increases to the supervised limit when increasing the dataset size (and even surpasses it slightly). This limit here is calculated through a supervised random forest on 1M training and test samples.

Interestingly, the separation quality is not monotonous but contains a surprisingly high value at 1000 samples. Our explanation for this is that these are so few samples that our second training step does not converge yet, not finding a worse solution.

But afterward, we see that our separation quality continuously grows as we have more measurements. The performance here does not reach perfect separation, as both distributions overlap, but almost reaches the supervised limit with 200000 samples and even surpasses it slightly.

This proves that we can reach supervised performance in the zero-supervised case as long as we have enough (unlabeled) measurements, making it useful for many applications where unlabeled data can easily be recorded. Still, we believe this not to be the only solution, and that it is possible to modify our approach also to work when anomalies are rare and few measurements were made. Intuitively, following our thought experiment, it might be possible to choose to "select both borders" and follow an unsupervised paradigm. But only as long as there is confusion. Thus, this would use *DOUST* only when it provides a benefit. To help with further development, we describe other approaches we have taken in the appendix.

This includes weighting the terms of our loss function to move the equilibrium described in Equation 4. Appendix F shows that weights do help to improve the performance in every case, but especially at low ν . Still, it is also not enough to cancel out the performance decrease.

Instead, in Appendix J, we describe our experiments with alternative loss functions. Notably is the function described in Appendix J.1, which is independent of the fraction of outliers in the test set ν . Sadly, this independence comes at the cost of lower overall performance and more complicated training.

5 Conclusion

In this paper, we are the first to explicitly maximize the difference between training and test distribution for outlier detection. As long as two conditions are fulfilled, this allows our algorithm *DOUST* to outperform competitive algorithms drastically. These conditions are

1. A clean training set, not containing anomalies; one-class classification
2. Enough unlabeled test samples ($N \gg \frac{1}{\nu^2}$)

If these conditions are fulfilled, *DOUST* is able to achieve supervised performance while using zero labeled anomalies. We believe the possible use cases of this to be immense. While many supervised fault detection algorithms work well on specific cases, complicated unsupervised/one-class algorithms are needed to catch unexpected errors with a lower success rate. Using our algorithm, we can also catch these unexpected errors with a performance that is competitive to the expected labeled errors. This fits well with the task of fraud detection. Given clean data, we are able to find arbitrary deviations that might not even have been thought of, with the only condition that this fraud happens enough. So even when a malicious actor is undetectable at first, he becomes detectable as long as he continues long enough. This can almost be seen as an upper limit on the amount of fraud possible before *DOUST* detects it.

But maybe the most exciting application is to science. Many fields search for anomalies in their measurements to be able to explain them later[33]. However, finding anomalies without a theory is hard, making them often go unnoticed [18]. Instead, we can find anomalies well, without any human biases or the need to explain them first. And because of the high availability of simulated (clean) datasets, we believe running *DOUST* on measurements can result in many interesting discoveries.

But we also do not believe our algorithm to be perfect yet. The space of possible loss functions is immense, and it is likely that there is one loss function that requires significantly less data (second condition), extending our possible applications even further. Similarly, we think it should be possible to soften also our first condition further. While we assume this here, we likely are never able to use perfectly clean training data. A difference in anomaly fraction between training and test data might also be more than enough (Appendix F). Finally, we only studied tabular data in this paper, as the best competitors and surveys handle tabular data. However, we believe our approach to be general enough to work on each type of data and so extending our algorithm to images, graphs, and especially data streams might pose their own challenges and create interesting, highly effective algorithms. We leave this for dedicated studies.

References

- [1] Arn Baudzus, Bin Li, Adnane Jadid, and Emmanuel Müller. On model performance estimation in time series anomaly detection. In *2023 6th International Conference on Computational Intelligence and Intelligent Systems*, 2023.
- [2] Jessa Bekker and Jesse Davis. Learning from positive and unlabeled data: a survey. *Machine Learning*, 109(4):719–760, Apr 2020.
- [3] Abdenour Bounsiar and Michael G. Madden. One-class support vector machines revisited. In *2014 International Conference on Information Science Applications (ICISA)*, pages 1–4, 2014.
- [4] Kendrick Boyd, Kevin H. Eng, and C. David Page. Area under the precision-recall curve: Point estimates and confidence intervals. In Hendrik Blockeel, Kristian Kersting, Siegfried Nijssen, and Filip Železný, editors, *Machine Learning and Knowledge Discovery in Databases*, pages 451–466, Berlin, Heidelberg, 2013. Springer Berlin Heidelberg.
- [5] Leo Breiman. Random forests. *Machine learning*, 45, 2001.
- [6] Markus Breunig, Peer Kröger, Raymond Ng, and Joerg Sander. Lof: Identifying density-based local outliers. volume 29, pages 93–104, 06 2000.
- [7] Benedikt Böing, Simon Klütermann, and Emmanuel Müller. Post-robustifying deep anomaly detection ensembles by model selection. In *ICDM*, 2022.
- [8] Sergei Chekanov and Walter Hopkins. Event-based anomaly detection for new physics searches at the LHC using machine learning. In *APS April Meeting Abstracts*, volume 2022 of *APS Meeting Abstracts*, page Q09.001, January 2022.
- [9] Jinghui Chen, Saket Sathe, Charu Aggarwal, and Deepak Turaga. *Outlier Detection with Autoencoder Ensembles*, pages 90–98. 06 2017.
- [10] LI Dong, LIU Shulin, and Hongli Zhang. A method of anomaly detection and fault diagnosis with online adaptive learning under small training samples. *Pattern Recognition*, 64, 2017.
- [11] Milton Friedman. A comparison of alternative tests of significance for the problem of \$m\$ rankings. *Annals of Mathematical Statistics*, 11:86–92, 1940.
- [12] Yossi Gandelsman, Yu Sun, Xinlei Chen, and Alexei A Efros. Test-time training with masked autoencoders. In Alice H. Oh, Alekh Agarwal, Danielle Belgrave, and Kyunghyun Cho, editors, *Advances in Neural Information Processing Systems*, 2022.
- [13] Cyril Goutte and Eric Gaussier. A probabilistic interpretation of precision, recall and f-score, with implication for evaluation. volume 3408, pages 345–359, 04 2005.
- [14] Xiaoyi Gu, Leman Akoglu, and Alessandro Rinaldo. Statistical analysis of nearest neighbor methods for anomaly detection. In Hanna M. Wallach, Hugo Larochelle, Alina Beygelzimer, Florence d’Alché Buc, Emily B. Fox, and Roman Garnett, editors, *NeurIPS*, pages 10921–10931, 2019.
- [15] Rajib Kumar Halder. Cardiovascular disease dataset, 2020.
- [16] Songqiao Han, Xiyang Hu, Hailiang Huang, Mingqi Jiang, and Yue Zhao. Adbench: Anomaly detection benchmark. In *NeurIPS*, 2022.
- [17] J.A. Hanley and Barbara Mcneil. The meaning and use of the area under a receiver operating characteristic (roc) curve. *Radiology*, 143:29–36, 05 1982.
- [18] N.R. Hanson. *The Concept of the Positron: A Philosophical Analysis*. Cambridge University Press, 1963.
- [19] Zengyou He, Xiaofei Xu, and Shengchun Deng. Discovering cluster-based local outliers. *Pattern Recognition Letters*, 24(9):1641–1650, 2003.
- [20] Megan L. Head, Luke Holman, Robert Lanfear, Andrew T. Kahn, and Michael D. Jennions. The extent and consequences of p-hacking in science. *PLoS Biology*, 13, 2015.
- [21] Waleed Hilal, S Andrew Gadsden, and John Yawney. Financial fraud: a review of anomaly detection techniques and recent advances. *Expert systems With applications*, 193, 2022.
- [22] Sture Holm. A simple sequentially rejective multiple test procedure. *Scandinavian Journal of Statistics*, 6(2):65–70, 1979.

[23] Shehroz S. Khan and Michael G. Madden. A survey of recent trends in one class classification. In Lorcan Coyle and Jill Freyne, editors, *Artificial Intelligence and Cognitive Science*, pages 188–197, Berlin, Heidelberg, 2010. Springer Berlin Heidelberg.

[24] Simon Klüttermann and Emmanuel Müller. Evaluating and comparing heterogeneous ensemble methods for unsupervised anomaly detection. In *IJCNN*, 2023.

[25] Aleksandar Lazarevic and Vipin Kumar. Feature bagging for outlier detection. volume 21, pages 157–166, 01 2005.

[26] Xiaoli Li, B. Liu, and See-Kiong Ng. Learning to identify unexpected instances in the test set. In *International Joint Conference on Artificial Intelligence*, 2007.

[27] Jian Liang, Ran He, and Tien-Ping Tan. A comprehensive survey on test-time adaptation under distribution shifts. *ArXiv*, abs/2303.15361, 2023.

[28] Fei Tony Liu, Kai Ming Ting, and Zhi-Hua Zhou. Isolation forest. In *ICDM*, 2008.

[29] Xiaofeng Liu, Chaehwa Yoo, Fangxu Xing, Hyejin Oh, Georges Fakhri, Je-Won Kang, and Jonghye Woo. Deep unsupervised domain adaptation: A review of recent advances and perspectives. *APSIPA Transactions on Signal and Information Processing*, 05 2022.

[30] Martin Q Ma, Yue Zhao, Xiaorong Zhang, and Leman Akoglu. The need for unsupervised outlier model selection: A review and evaluation of internal evaluation strategies. *ACM SIGKDD Explorations Newsletter*, 25(1), 2023.

[31] Viktor Malyi. Run or walk dataset, Jul 2017.

[32] Federico Di Mattia, Paolo Galeone, Michele De Simoni, and Emanuele Ghelfi. A survey on gans for anomaly detection, 2021.

[33] Vinicius Mikuni, Benjamin Nachman, and David Shih. Online-compatible unsupervised nonresonant anomaly detection. *Phys. Rev. D*, 105:055006, Mar 2022.

[34] Dubravko Miljković. Fault detection methods: A literature survey. In *2011 Proceedings of the 34th International Convention MIPRO*, pages 750–755, 2011.

[35] Isaac Monroy, Gerard Escudero, and Moisès Graells. Anomaly detection in batch chemical processes. In Jacek Jeżowski and Jan Thullie, editors, *19th European Symposium on Computer Aided Process Engineering*, volume 26 of *Computer Aided Chemical Engineering*, pages 255–260. Elsevier, 2009.

[36] Huiyu Mu, Ruizhi Sun, Gang Yuan, and Guoqing Shi. Positive unlabeled learning-based anomaly detection in videos. *International Journal of Intelligent Systems*, 36, 05 2021.

[37] Madalina Olteanu, Fabrice Rossi, and Florian Yger. Meta-survey on outlier and anomaly detection. *Neurocomputing*, 555:126634, 2023.

[38] Fabian Pedregosa, Gaël Varoquaux, Alexandre Gramfort, Vincent Michel, Bertrand Thirion, Olivier Grisel, Mathieu Blondel, Peter Prettenhofer, Ron Weiss, Vincent Dubourg, et al. Scikit-learn: Machine learning in python. *Journal of machine learning research*, 12(Oct):2825–2830, 2011.

[39] Chen Qiu, Aodong Li, M. Kloft, Maja R. Rudolph, and Stephan Mandt. Latent outlier exposure for anomaly detection with contaminated data. In *International Conference on Machine Learning*, 2022.

[40] Payam Refaeilzadeh, Lei Tang, and Huan Liu. *Cross-Validation*, pages 532–538. Springer US, Boston, MA, 2009.

[41] Lukas Ruff, Jacob Kauffmann, Robert Vandermeulen, Gregoire Montavon, Wojciech Samek, Marius Kloft, Thomas Dietterich, and Klaus-Robert Müller. A unifying review of deep and shallow anomaly detection. *Proceedings of the IEEE*, PP:1–40, 02 2021.

[42] Lukas Ruff, Robert Vandermeulen, Nico Goernitz, Lucas Deecke, Shoaib Ahmed Siddiqui, Alexander Binder, Emmanuel Müller, and Marius Kloft. Deep one-class classification. In *ICML*, 2018.

[43] Lukas Ruff, Robert A. Vandermeulen, Nico Görnitz, Alexander Binder, Emmanuel Müller, Klaus-Robert Müller, and Marius Kloft. Deep semi-supervised anomaly detection. *CoRR*, abs/1906.02694, 2019.

- [44] Mayu Sakurada and Takehisa Yairi. Anomaly detection using autoencoders with nonlinear dimensionality reduction. In *Proceedings of the MLSDA 2014 2nd Workshop on Machine Learning for Sensory Data Analysis*, MLSDA’14, page 4–11, New York, NY, USA, 2014. Association for Computing Machinery.
- [45] Yu Sun, Xiaolong Wang, Zhuang Liu, John Miller, Alexei A. Efros, and Moritz Hardt. Test-time training with self-supervision for generalization under distribution shifts. In *Proceedings of the 37th International Conference on Machine Learning*, ICML’20. JMLR.org, 2020.
- [46] Kai Tian, Shuigeng Zhou, Jianping Fan, and Jihong Guan. Learning competitive and discriminative reconstructions for anomaly detection. In *AAAI Conference on Artificial Intelligence*, 2019.
- [47] Frank Wilcoxon. Individual comparisons by ranking methods. *Biometrics Bulletin*, 1(6):80–83, 1945.
- [48] Xueying Zhan, Qingzhong Wang, Kuan-Hao Huang, Haoyi Xiong, Dejing Dou, and Antoni B. Chan. A comparative survey of deep active learning. *ArXiv*, abs/2203.13450, 2022.
- [49] Jiaqi Zhang, Zhenzhen Wang, Junsong Yuan, and Yap-Peng Tan. Positive and unlabeled learning for anomaly detection with multi-features. pages 854–862, 10 2017.
- [50] Yue Zhao and Maciej K. Hryniwicksi. Xgbod: Improving supervised outlier detection with unsupervised representation learning. In *2018 International Joint Conference on Neural Networks (IJCNN)*. IEEE, July 2018.
- [51] Yue Zhao, Zain Nasrullah, and Zheng Li. Pyod: A python toolbox for scalable outlier detection. *Journal of Machine Learning Research*, 20(96):1–7, 2019.

A Experimental Setup

A.1 Model Characteristics

Our models use a neural network ($f(x)$) built from three layers with 100 nodes and one output layer with 1 node. Following [42, 7], all layers use no bias term. Every layer except the last one is activated with a relu activation; the last one instead uses the modified sigmoid activation, as shown in Equation 2. We use a sigmoid-like activation because a fixed output range simplifies our loss, but we have to shift its values slightly to make sure the function $sigmoid(0) = \frac{1}{2}$ is not a trivial solution.

This network is trained in two steps. In the first training step, we only consider training data and minimize the DEAN-like ([7]) loss in Equation 1: Every (training) sample should be mapped close to $f(x) = \frac{1}{2}$, so close to the center of the available output range. For this optimization, we use 5 epochs and a batch size of 100. We did only slightly optimize these parameters (Appendix H) and think there are likely better values that could be chosen, but we also don't believe them to affect our results strongly. This first training step results in all samples being mapped into a range that we can optimize easily (there is no $f(x) \approx 0, 1$). Additionally, the output values are close to each other for normal samples. This already works as an outlier detector ([7]), but works drastically worse when compared to the second optimization step. We choose a low number of epochs here, as having learned imperfect representations seems to allow the second step to change our predictions more easily.

For this second training step, in which we also use test-time data (and which thus can only be done as part of the evaluation), we declare labels of 0 for each training sample and 1 for each test sample and try to minimize the distance between label and function output $f(x)$. This is done, for example, with the loss function given in Equation 3, or the other loss functions studied in Appendix J. Here, we train for 50 epochs with the same batch size of 100. During the second training loop, we expect normal samples to be pulled to a low value and abnormal samples to the maximum value of 1. This means that after training, we can use the function output $f(x)$ as an indicator of outlierness: The higher $f(x)$, the more likely x is an outlier.

A.2 Ensembles

Instead of comparing the performance of a singular model, we combine 100 models into an ensemble:

$$F(x) = \frac{1}{100} \sum_{i=1}^{100} f_i(x) \quad (6)$$

This averages out slightly worse neural network initializations, making our results more reproducible and increasing their performance slightly. We chose to combine 100 models, as this is the same number of models as are used by the isolation forest competitor. Ensembles are studied in the ablation study in Appendix G.1.

A.3 Simulated Experiment Setup

The experiment in Figure 6 requires simulated data. Simulated data allows us to change the size of the test set in arbitrary ranges and still compare different test sets fairly.

We choose data that is sampled from a ground truth Gaussian distributions in ten dimensions. The normal samples have a mean of $\mu = \vec{0}$ and standard deviation of $\sigma = \vec{1}$. The outlier samples follow a similar distribution centered around $\mu = \vec{1}$.

On a training set of N samples and a test set build from $0.99 \cdot N$ normal samples and $0.01 \cdot N$ outliers, we train our algorithm (As described in Appendix A.1). We ignore the small performance gain described in Appendix G.1, and train just one submodel for each ensemble. Instead, we train models on 1000 differently sampled datasets for each value of N and average their performance (compared to their predictions as in the ensemble). This removes uncertainties that we get from the random generation of samples. These are especially critical for low N ; for the minimum value of $N = 1000$, we only generate $1000 \cdot 1\% = 10$ anomalies. This means a single sample randomly overlapping with the normal distribution can result in a difference of 5% in ROC-AUC (see Appendix C.1).

For our competitor, we choose a random forest trained on the maximum number of samples studied for our algorithm (one million). This algorithm is repeated ten times, and the performance is averaged, even though the repetition uncertainty is neglectable.

B Comparison Algorithms

B.1 Unsupervised Algorithms

We choose our competitor algorithms following a recent survey [16]. We take the three best algorithms: An isolation forest (ifor) [28], a k-nearest neighbor algorithm (knn) [14], and a cluster-based extension of the local outlier factor (cblof) [19]. While many more algorithms are possible, we want to keep the number of algorithms limited (increasing the number of algorithms increases the critical difference needed for a significant difference). Following the survey, many more algorithms perform only statistically insignificantly worse than these three algorithms, and thus, we can not say that these algorithms are the best on general data. But since we also use datasets from the same survey, we can say that these are likely the best-performing algorithms on these commonly used datasets. Following this reasoning results in us only using shallow competitors but comparing them to a deep learning method. However, as clearly shown in the survey, using deep learning competitors would only result in an even more significant difference between DOUST and the competitors.

We also use the same implementation as used in the survey. It is implemented in pyod [51], and we follow standard hyperparameters. The exception is the knn algorithm, where changing the number of nearest neighbors considered from $k = 5 \rightarrow k = 1$ improves this competitor's performance [14].

B.2 Supervised Algorithms

We use a supervised algorithm not as a competitor but more as an upper limit for outlier detection algorithms. When an algorithm does not have access to any labels, how can it perform better than one that has labels? But in practice, there are two reasons why this does not have to be the absolute upper limit. Training on highly imbalanced data can result in trivial optima, and test time training can allow us to specify our model to work best on the specific test data used.

Since supervised test time classification methods are not reliable enough to be a viable competitor, especially when considering limited data, we accept that our limit might not be absolute. And as Figure 6 shows, we are able to outperform it (even when the data is not imbalanced).

To work with the imbalanced data, we choose to use a random forest algorithm[5] as our supervised algorithm. We use the sklearn implementation [38] with standard hyperparameters. A random forest works well with low amounts of data (allowing us to learn only on the test set), and the invariance to normalization also makes training them more reliable. We also considered comparing this against the best semi-supervised algorithm from the previously mentioned survey, XGBOD [50], but chose not to do so, as the performance is worse than the supervised algorithm.

Similarly, we do not compare against PU-learning approaches. PU-learning approaches for outlier detection tasks are rare, and thus, there is no agreement in the community on a viable comparator. Our implementation of [49] does barely reach a comparison performance comparable to our unsupervised competitors.

B.3 Crossvalidation

With exception of the unsupervised algorithms, the other algorithms require access to labeled anomalies. Since we only have anomalies in our test set, we also have to use this set for training. This can result in overfitting and an unfair comparison. To solve this, we use cross-validation [40]. We equally distribute every normal and abnormal sample in the test set into five equally sized groups. Then we train five models, where each model is trained on four datasets, and make predictions for the fifth. These predictions are combined, and we calculate the ROC-AUC on the combined dataset.

C ROC-AUC and Datasplits

Outlier detection is usually evaluated with one of three metrics. Next to the ROC-AUC[17], the AUCPR [4] and the F1-Score [13] are also commonly used. But for our analysis, only the ROC-AUC can be used, which is what we want to show here.

The F1-Score can not be used since it requires boolean predictions (either normal or outlier, not an outlier score like we and our competitors give). While we can convert outlier scores into these boolean predictions by using a threshold, this requires consistently choosing comparable, highly efficient thresholds. This makes every comparison much harder since a badly performing algorithm might only perform badly because its predictions make it harder to choose this threshold. Also, the reliance on boolean inputs generally increases the repetition uncertainty.

We can also not use the AUCPR because this metric depends on the fraction of anomalies in the test set (ν). And since we directly measure the change in performance of our algorithm when changing ν , we want to make sure that we can separate performance changes from changes in our evaluation metric.

Luckily, the ROC-AUC metric fulfills both requirements, being invariant to ν and working with continuous outlier scores. Still, that does not mean that the ROC-AUC is perfect for our analysis (See Appendix C.1).

C.1 ROC-AUC biases

While the ROC-AUC is the only common metric invariant under the fraction of anomalies in the training set ν , making it invaluable for our analysis, this does not mean it is perfect. One drawback that we want to mention here is the difference in handling false positives and false negatives.

The ROC-AUC $roc(A, B)$ is defined as the probability of a random value in B being higher than a random value in A . To illustrate the difference, we assume the existence of worst-case samples: $w_B < a \forall a \in A$ and $w_A > b \forall b \in B$. We further use $N_{A/B} = \|A/B\|$ to represent the number of samples in A/B . Using the attributes discussed in Appendix D, we find:

$$roc(A + w_A, B) = \frac{N_A}{N_A + 1} roc(A, B) \quad (7)$$

and

$$roc(A, B + w_B) = \frac{N_B}{N_B + 1} roc(A, B) \quad (8)$$

So, when adding worst-case samples, the ROC-AUC changes by $\frac{1}{N_{A/B} + 1}$. This is asymmetric since anomalies are usually rare, and thus $N_A \gg N_B$.

Missing an anomaly (false negative) is punished significantly more than considering a normal point as abnormal (false positive). Because this difference disappears as long as the fraction of anomalies in the test set is $\nu = \frac{1}{2}$, it is generally a good idea to split a dataset in such a way.

In Figure 5, the green line performs at least similarly well to the blue line. But if we calculate the total number of mistaken samples, this changes, as the green line consistently makes the most mistakes.

The green line finds false positives on both sides. Resulting in, on average, $2 \cdot N \cdot f$ mistakes. A blue model, in the worst case where it only guesses, still picks the right side half of the time, resulting in $N \cdot f + \frac{A}{2}$ mistakes. So the green line makes more mistakes, as long as $N \cdot f > \frac{A}{2}$. In our example $A = 20$ and $f \approx 0.023$. So for $N > \frac{20}{2 \cdot 0.023} \approx 435$, the green line makes the most mistakes, even when the blue model does not work at all. For smaller values, the blue AUC is higher than the green one, implying that the most mistaken samples in our thought experiment are consistently made by the more classical green algorithm.

D Using the ROC-AUC for model selection

There is a relation between the ROC-AUC between the training and test dataset and the ROC-AUC between the normal and abnormal parts of the test set.

For this, we assume we have data following two distributions. p_{normal} for normal samples and $p_{abnormal}$ for the outliers.

The training set T contains N_{train} samples, while the test set E contains $N_{test} = N + O$ samples. Here $\frac{O}{N+O} = \nu$ is the fraction of anomalies in the test set.

The ROC-AUC $roc(A, B)$ is defined as the probability that a random element of B is higher than A . This implies three important attributes.

$$roc(A, A) = \frac{1}{2} \quad (9)$$

$$roc(A, B + C) = \frac{\|B\|}{\|B\| + \|C\|} roc(A, B) + \frac{\|C\|}{\|B\| + \|C\|} roc(A, C) \quad (10)$$

$$roc(A, B + B) = roc(A, B) \quad (11)$$

This allows us to rewrite

$$\begin{aligned} ROC_{train/test} &= roc(T, E) = roc(p_{normal}, (1 - \nu) \cdot p_{normal} + \nu \cdot p_{abnormal}) \\ &= \frac{N}{N + O} \cdot roc(p_{normal}, p_{normal}) + \frac{O}{N + O} \cdot roc(p_{normal}, p_{abnormal}) = \frac{1 - \nu}{2} + \nu \cdot ROC_{normal/abnormal} \end{aligned}$$

So, the difference between the ROC-AUC of training and test set, and the ROC-AUC score of normal and abnormal samples is a linear relationship (ν is a constant for a given dataset). When $\nu \rightarrow 0$, $ROC_{train/test} \rightarrow \frac{1}{2}$ regardless of $ROC_{normal/abnormal}$ and so small uncertainties resulting from differences between training and test distribution can dominate the calculation. These uncertainties stem from the fact two datasets sampled from the same distribution only fulfill Equation 9 if infinite samples are drawn. Thus, similarly to our experiments in Section ??, these uncertainties disappear when enough samples are used.

This solves another problem in outlier detection: Since usually no outliers are known, it is not possible to evaluate how well a certain model performs. Thus, tasks like model selection or hyperparameter optimization are (almost) impossible [30]. So, most applications have to rely on only limited experience when choosing their models, likely resulting in often subpar performance. But having a metric, like the $ROC_{train/test}$, that can be calculated without knowledge of outliers can solve this since when choosing the algorithm/hyperparameter combination with the better metric, it also means it has a better outlier performance.

This likely could be used to improve our algorithm further by optimizing its hyperparameters for each dataset. We have not studied this here.

E Drawbacks of upsampling

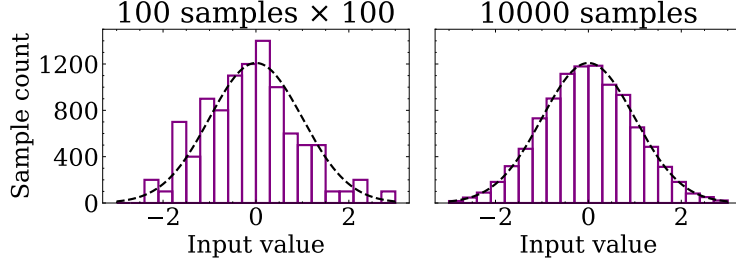


Figure 7: Two datasets sampled from the same distribution. The left one is upsampled 100 times while the right contains 100× more samples.

As described in Section ??, downsampling our data has a significant impact on our detection quality. In fact, the effect is more significant compared to practical applications since we decrease both the fraction of anomalies in the test set and the size of our dataset. Both actions make our algorithm work worse. Additionally, this forces us to remove some datasets which contain too few anomalies (16 of 47, see Section 3.2).

This implies the question of why we do not simply upsample the existing normal data to reach the same anomaly fraction in the test set. Consider the samples shown in Figure 7: When repeating samples, they do not follow the same distribution as when generating new data. In particular, outliers are handled imperfectly, as they can get multiplied (right side) or stay absent (left side).

So while the separation between normal and abnormal samples might be more favorable (see the start of Section ??), the problem of outliers not being clearly defined stays the same when we upsample a dataset. And since this does not happen in real data, we choose to use downsampling to be more realistic.

Similarly, we can not move samples from the training set to the test set, since this would mean that also the performance of our competitors changes. Also, this would not allow reaching values of $\nu = 1\%$ consistently, since the training set is limited.

F Weighting loss terms

We can adapt Equation 3, by introducing a weighting factor ω to the :

$$L = \frac{1}{\|X_{train}\|} \sum_{x \in X_{train}} x^2 + \omega \cdot \frac{1}{\|X_{test}\|} \sum_{x \in X_{test}} (1-x)^2 \quad (12)$$

This modifies our optimal separation (Similar to Equation 4 we again assume $\|X_{train}\| = \|X_{test}\| \rightarrow \infty$)

$$L \propto \int_{\mathcal{R}^d} dx p_{normal}(x) \cdot (f(x)^2 + \omega \cdot (1-\nu) \cdot (1-f(x))^2) + p_{abnormal} \cdot \omega \cdot \nu \cdot (1-f(x))^2 \quad (13)$$

This loss is minimal when $f(x) = 1$ for all abnormal samples, and $f(x) = \frac{1-\nu}{1+\frac{1}{\omega}-\nu}$ for all normal ones. This means, in the optimal case, normal and abnormal samples are separated by $\Delta = \frac{1}{1+\omega-\nu\omega}$, which is larger than the unweighted separation ($\Delta = \frac{1}{2-\nu}$) as long as $\omega < 1$.

Since the separation, and thus the difference between normal and abnormal samples, is minimal, when anomalies are rare, this can counteract one effect that makes *DOUST* work worse for low ν . We evaluate this experimentally in Figure 8.

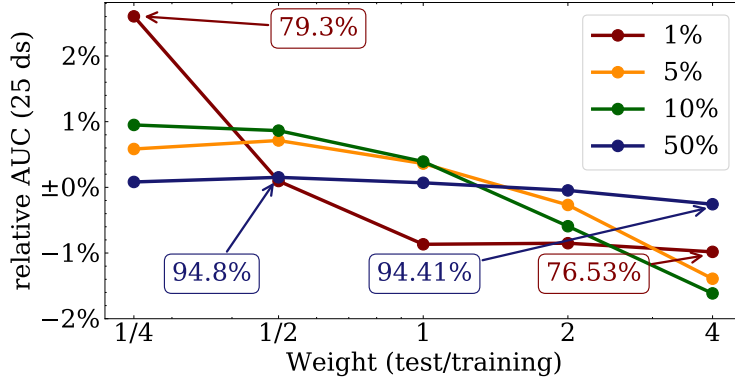


Figure 8: Average ROC AUC, relative to the average $(\frac{auc - mean(auc)}{mean(auc)})$, for different values of ν (legend) and different weights ω (x axis).

As expected, we see a lower weight increasing the outlier detection performance. Additionally, this effect is stronger the lower ν is, with a $> 3\%$ change for $\nu = 1\%$, but a $\approx \frac{1}{2}\%$ change when $\nu = 50\%$.

While it seems to be possible to increase the performance even further by choosing smaller and smaller weights, the magnitude of this effect is simply not strong enough to make models trained on various ν values comparable.

Especially since training with the lowest value of ν is not always optimal. A low ν means that the second term in the loss 12 can be neglected with lower cost, resulting in the local minima of $f(x) = 0$ becoming more likely (Even though for all $\omega > 0$ this is still only a local minima). Additionally, we always assume that our training data is entirely normal, but in practice, it might also be slightly contaminated (with a fraction $\gamma < \nu$). This would modify our loss calculation to:

$$L \propto \int_{\mathcal{R}^d} dx p_{normal}(x) \cdot ((1-\gamma) \cdot f(x)^2 + \omega \cdot (1-\nu) \cdot (1-f(x))^2) + p_{abnormal} \cdot (\gamma \cdot f(x)^2 + \omega \cdot \nu \cdot (1-f(x))^2) \quad (14)$$

Which is minimal when $f(x) = \frac{\omega \cdot (1-\nu)}{1+\omega(1-\nu)-\gamma}$ for all normal samples and $f(x) = \frac{\nu \cdot \omega}{\gamma+\nu \cdot \omega}$ for all abnormal ones, and thus $\Delta = \frac{(\nu-\gamma) \cdot \omega}{(1+\omega-\gamma-\omega \cdot \nu)(\omega \cdot \nu+\gamma)}$. Here, an as low as possible value of ω is no longer optimal. For example, when we assume $\nu = 0.1$ and $\gamma = 0.01$, the optimal value of ω is $\frac{\sqrt{11}}{10} \approx 0.33$.

This can also be seen in Figure 8, where the optimal weight for $\nu = 5\%$ and $\nu = 50\%$ is $\omega = \frac{1}{2} > \frac{1}{4}$.

Choosing the right weighting factor is a way for DOUST to be further optimized, especially since Appendix D allows finding this hyperparameter without knowing outlier. But as this would greatly increase both runtime and complexity while likely only providing marginal improvements, we leave this for further study.

Using these results, it might also be possible to estimate the fraction of anomalies in both training and test set (γ and ν), but we have not studied this.

G Ablation Studies

G.1 Ensemble Use

To justify parts of our model setup, we add two ablation studies. The first one considers whether it is useful to combine multiple models into an ensemble, or if we should consider only the performance of one submodel.

In unsupervised learning, deep ensembles generally provide assurance against suboptimal initializations [24], and here they also behave similarly. In Figure 9, we show that the ensemble improves the model a bit but also that this improvement is not very strong. The biggest improvement is seen for low values of the anomaly fraction ν , where the submodels have the highest uncertainty.

We use ensembles in this paper, as we aim to have the best possible results, but in practice (or for simpler tasks, like in Figure 6), the runtime increase of a factor 100 might not be justified by a small improvement.

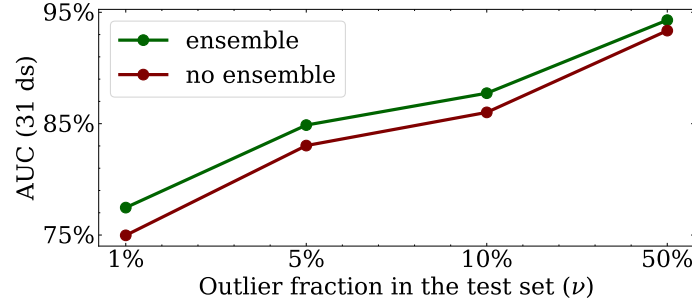


Figure 9: Average ROC-AUC performance when using ensembles, compared to when not using an ensemble.

G.2 Feature Bagging

Additionally, in contrast to the original DEAN paper [7], we suggest not using feature bagging [25]. To justify this, we also compare this performance to the one we would reach with 50% feature bagging in Figure 10 (each submodel randomly has access to half the features).

The decrease is more significant here, no longer performing comparably to the supervised algorithm. We think this is the case since often only some features allow for separation, and thus, a high fraction of models can only learn possibly counterproductive separations.

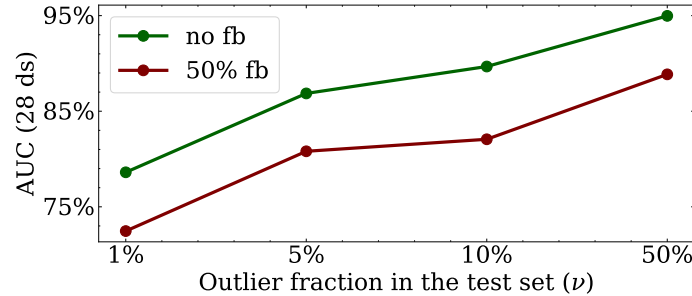


Figure 10: Average ROC-AUC performance when using or not using feature bagging (here 50% of features are used for each submodel)

H P-hacking and Repetition Problems

A common problem in papers like ours is p-hacking[20]. We only consider a threshold of 5% to find a significant improvement. Thus, when testing approximately 20 independent models, it is likely that we will accidentally find something that looks significant. And since many hyperparameters need to be chosen, and many different loss functions are possible (See Appendix J), this might become a real problem for us.

And while we think that our performance is more than accidental, here we want to describe our approach to guarantee this briefly.

Namely, we minimized the repetition problems of three effects.

H.1 Hyperparameters

To limit how optimized our hyperparameters are on the datasets we use, we first choose a high number of different datasets to make the existence of a local optimum less likely.

But maybe more importantly, we do not optimize hyperparameters on these datasets at all. Instead, we select another, unrelated dataset on which we experiment to make our algorithms work well. Later, we only apply and evaluate this algorithm once on the evaluation datasets.

For this, we chose the RunOrWalk dataset [31]. As it is originally designed for classification, we use half of all "walking" samples as training data and try to find the "running" samples from the remaining set. This dataset is optimal for our optimizations, as it contains over 88000 samples, half of which are abnormal, allowing for meaningful resampling. Additionally, "running" samples are relatively evenly distributed, decreasing the randomness of our classification performance.

H.2 Loss functions

Similarly, we also evaluate only one loss function on the evaluation datasets for the conclusions of the main paper. While further loss functions can be found in Appendix J, these are not used to evaluate the usefulness of our approach but were only tested after we found significant results in our main experiments, to understand our approach further.

H.3 Dataset choices

To not bias the selection of datasets, we follow the dataset choices of a recent survey [16]. Still, we restrict ourselves to only using their "classical" datasets because of computational cost considerations (See Appendix I). Especially since using the rest of their datasets increases not only the cost and complexity of each model but they are also less interesting since we would construct multiple highly correlated tasks from the same data and these are originally classification datasets.

I Computational cost considerations

In total, this paper required training more than 300000 *DOUST* models. While some combinations fail early, through to the reasons outlined in Section 3.2, this also means training more models to assert that we have enough information.

Training a model depends on the dataset's size, but a rough estimate of one minute of GPU time is reasonable. We use an NVIDIA A100 graphics card with 40GB of VRAM, resulting in about 30 weeks of computation time.

Because of this high cost, we leave further modifications, as the one suggested in Appendices F and D for dedicated studies.

J Comparison of loss functions

J.1 A fraction independent loss

One idea to create a model that does depend less on the fraction of anomalies in the test set ν , is to use a loss function that does not change when we change ν .

For this, we search for a distance function $d(A, B)$ between datasets A and B that fulfills three axioms.

Our first axiom is scale invariance (Equation 15). When changing the size of a dataset, without changing its distribution, $d(A, B)$ is not affected.

$$d(A, \nu \cdot B) = d(A, B) \quad (15)$$

Our second axiom is an addition law, in 16.

$$d(A, B + C) = \max(d(A, B), d(A, C)) \quad (16)$$

This equation allows us to ignore the normal samples in the test set, and only focus on the abnormal ones. (See Appendix D, for an example of a function, the ROC-AUC, which fulfills Equation 15, but not this axiom and the problems associated with this)

And finally, we assume asymmetry in Equation 17. Demanding asymmetry allows us to narrow down the list of potential functions and simplifies our calculations, but is not necessarily needed this strongly.

$$d(A, B) = -d(B, A) \text{ and thus also } d(A, A) = 0 \quad (17)$$

If we find a function $d(A, B)$ that fulfills these axioms, we can infer a loss function $L = -d(X_{train}, X_{test})$ that is independent of the fraction of anomalies in the test set.

Proof.

$$\begin{aligned} L_d &= -d(X_{train}, X_{test}) = -d(X_{train}, (1 - \nu) \cdot X_{normal} + \nu \cdot X_{abnormal}) \\ &= -\max(d(X_{train}, X_{normal}), d(X_{train}, X_{abnormal})) = -\max(d(X_{train}, X_{abnormal})) \end{aligned} \quad (18)$$

□

A simple distance function, that (almost) fulfills all three axioms, is

$$d(A, B) = \max(A) - \max(B) \quad (19)$$

Proof. Equation 15: $d(A, \nu \cdot B) = \max(A) - \max(\nu \cdot B) = \max(A) - \max(B) = d(A, B)$ (Technically, this assumes that the highest values in B and $\nu \cdot B$ are the same. This is usually only true if the distribution has no tails, and $\|A\|, \|B\| \rightarrow \infty$. But in practice they are at least close, which is enough to construct a loss function from this.)

Equation 16: $d(A, B + C) = \max(A) - \max(B + C) = \max(A) - \min(\max(B), \max(C)) = \max(\max(A) - \max(B), \max(A) - \max(C)) = \max(d(A, B), d(A, C))$

Equation 17: $d(A, B) = \max(A) - \max(B) = -(\max(B) - \max(A)) = -d(B, A)$

□

We test this loss experimentally. For this, we also extend our usual batch size from $100 \rightarrow 500$ to account for possible differences from not fulfilling our first axiom exactly.

The resulting comparison can be seen in Figure 11. While the performance seems indeed to be stable under changes of the outlier fraction, the total performance is also only average when compared with our competitors.

There might be another function fulfilling our axioms that produces a better performance. A simple way to extend our loss is to change $d(A, B) = \max(A) - \max(B)$ to $d(A, B) = \max(f(A)) - \max(f(B))$ with any function $f(x)$ as this similarly fulfills our axioms.

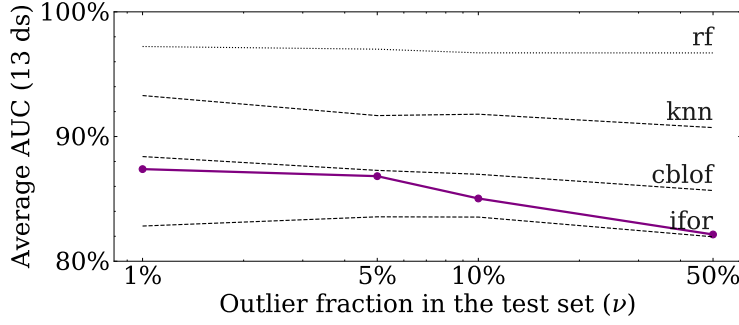


Figure 11: Performance of our algorithm, when using fraction independent loss, as a function of the fraction of anomalies in the test set. Our competitors are shown in the background.

J.2 Alternative losses considered

In this section, we list other loss functions that we at some point considered. This allows us to show how our algorithm’s performance changes when using different losses, hopefully contributing to a better understanding of how test-time training outlier detection works.

Next to the losses mentioned here, we also briefly considered a mean average error, and a loss similar to L_d replacing \max by \min . Both were not studied further, as their initial performance was significantly worse.

MSE

The loss function discussed in the main paper is very similar to a Mean-Squared Error loss when assuming the label for training data to be 0 and for test data to be 1. As a kind of ablation study, we also study an unmodified mse loss:

$$L_{mse} = \sum_{x \in X_{train}} f(x)^2 + \sum_{x \in X_{test}} (1 - f(x))^2 \quad (20)$$

As Figure 12 shows, the behavior is basically the same as in Figure 3, and so the difference can easily be neglected. This can also be seen by looking at the loss term weighting studied in Appendix F, since the difference between both loss functions is similar to a weighting term, which depends on the difference in size between the training and test set. But we still think that Equation 3 represents the better choice, since in real-world examples, there might be drastically more significant differences between the size of the training and test set and averaging each part allows to easier control this.

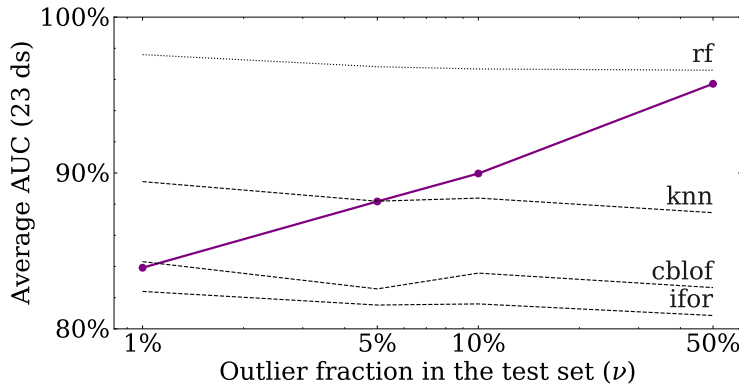


Figure 12: Performance of our algorithm, when using an unmodified mse loss, as a function of the fraction of anomalies in the test set. Our competitors are shown in the background.

mse+mae

While a mean average loss does not perform well and was quickly discarded, we still think that a loss that is more susceptible to small differences could be useful. For this, we study the sum of a mse and a mae loss:

$$L_{mse+mae} = \frac{1}{\|X_{train}\|} \sum_{x \in X_{train}} (x + x^2) + \frac{1}{\|X_{test}\|} \sum_{x \in X_{test}} ((1 - x) + (1 - x)^2) \quad (21)$$

But as Figure 13 shows, the effects are also minor at most, and the performance is slightly worse.

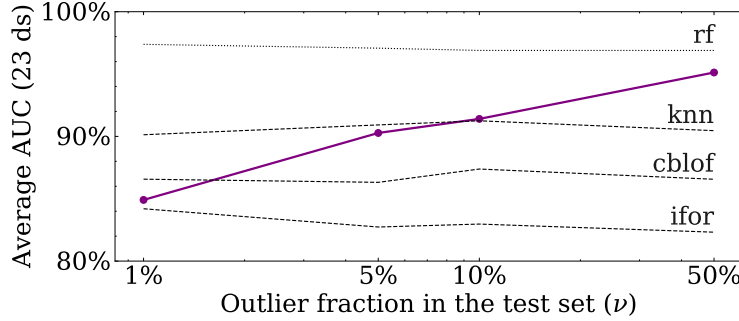


Figure 13: Performance of our algorithm, when using mse+mae loss, as a function of the fraction of anomalies in the test set. Our competitors are shown in the background.

Unmoving normal loss

Our usual loss requires both the prediction of normal and the prediction of abnormal samples to change in the second training step (during evaluation). When we set the expected value of normal samples to $\frac{1}{2}$, the prediction of no sample in the training set would need to change during the second training phase, potentially simplifying the training procedure.

$$L_{unmoving} = \frac{1}{\|X_{train}\|} \sum_{x \in X_{train}} \|x - \frac{1}{2}\| + \frac{1}{\|X_{test}\|} \sum_{x \in X_{test}} (1 - x) \quad (22)$$

But as Figure 14 shows, this also does not change much.

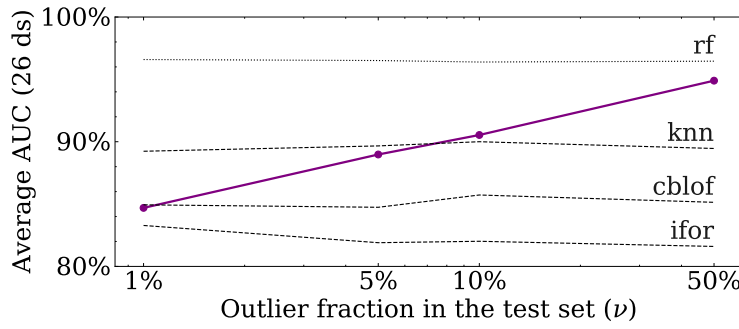


Figure 14: Performance of our algorithm, when using unmoving normal loss, as a function of the fraction of anomalies in the test set. Our competitors are shown in the background.

MeanMax Loss

Finally, the combination of both a fraction-independent *max* loss (that more strongly punishes high deviations) for the training samples, and an average (which can easily be separated into a normal and an abnormal part) for the test set, can provide interesting results:

$$L_{meanmax} = \max_{x \in X_{train}} x + \frac{1}{\|X_{test}\|} \sum_{x \in X_{test}} (1 - x) \quad (23)$$

As Figure 15 indicates, while the performance is only average for low ν , it stays stable. And while the performance of $\nu = 50\%$ is not as good as when using Equation 3 as a loss function, it is still better than all unsupervised competitors. A similar approach could allow using test data to specialize predictions when it is useful but to rely on unspecialized separation when it is not.

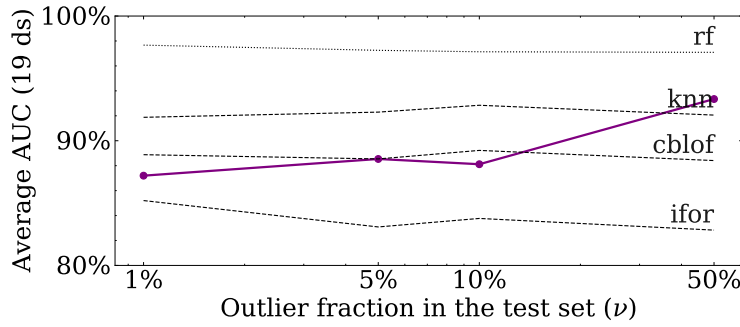


Figure 15: Performance of our algorithm, when using meanmax loss, as a function of the fraction of anomalies in the test set. Our competitors are shown in the background.

K Tabular algorithm comparison

	ifor	cblof	knn	doust	supervised	Normal	Outlier	Features
yeast	0.4012	0.4678	0.4462	0.7262	0.7921	977	507	8
WPBC	0.5373	0.507	0.5392	0.656	0.6686	151	47	33
speech	0.5402	0.4872	0.5031	0.7396	0.7354	3625	61	400
vertebral	0.4556	0.4333	0.4044	0.8911	0.8489	210	30	6
Wilt	0.4497	0.3628	0.5572	0.9941	0.9831	4562	257	5
ALOI	0.5594	0.5584	0.7099	0.7606	0.8539	48026	1508	27
Pima	0.7257	0.7036	0.7451	0.7361	0.8133	500	268	8
Hepatitis	0.7751	0.6331	0.7337	0.8107	0.8609	67	13	19
fault	0.6556	0.7031	0.807	0.8243	0.8757	1268	673	27
landsat	0.5673	0.7008	0.7698	0.9542	0.9621	5102	1333	36
campaign	0.7347	0.6764	0.7435	0.8827	0.9404	36548	4640	62
InternetAds	0.4526	0.8422	0.8735	0.9085	0.9596	1598	368	1555
celeba	0.729	0.7465	0.624	0.9713	0.966	198052	4547	39
letter	0.6258	0.8053	0.8856	0.9499	0.8712	1500	100	32
Cardiotocography	0.7804	0.7464	0.7694	0.9578	0.9842	1648	466	21
magic.gamma	0.7705	0.7872	0.8538	0.9208	0.9325	12332	6688	10
SpamBase	0.8242	0.7554	0.7892	0.9257	0.9824	2528	1679	57
satellite	0.7799	0.8867	0.8753	0.9545	0.9747	4399	2036	36
smtp	0.9122	0.83	0.93	0.8378	0.985	95126	30	3
mammography	0.8817	0.8526	0.876	0.9495	0.9555	10923	260	6
annthyroid	0.9276	0.743	0.8859	0.9956	0.9965	6666	534	6
optdigits	0.7249	0.8824	0.9994	0.9997	1.0	5066	150	64
backdoor	0.7749	0.9243	0.951	0.9858	0.9997	93000	2329	196
mnist	0.8603	0.874	0.9376	0.9872	0.9948	6903	700	100
vowels	0.7844	0.938	0.9788	0.9924	0.9694	1406	50	12
Ionosphere	0.8529	0.9351	0.9606	0.98	0.9705	225	126	32
wine	0.86	0.95	0.94	1.0	0.97	119	10	13
Stamps	0.9116	0.9386	0.9448	0.9854	0.9719	309	31	9
PageBlocks	0.9209	0.9145	0.9496	0.9832	0.992	4883	510	10
cover	0.8472	0.9497	0.9959	1.0	1.0	283301	2747	10
skin	0.8829	0.9188	0.9983	0.9994	1.0	194198	50859	3
Lymphography	1.0	1.0	1.0	1.0	0.8194	142	6	18
cardio	0.9497	0.9514	0.9397	0.9929	0.9969	1655	176	21
fraud	0.9569	0.9569	0.9727	0.9773	0.9819	284315	492	29
donors	0.9231	0.9309	1.0	1.0	1.0	582616	36710	10
WBC	0.99	0.99	0.99	0.97	0.96	213	10	9
glass	0.9259	1.0	1.0	0.9877	1.0	205	9	7
pendigits	0.9744	0.9675	0.9984	1.0	0.9992	6714	156	16
thyroid	0.9913	0.9679	0.9858	0.9985	1.0	3679	93	6
breastw	0.9967	0.9945	0.9941	0.9884	0.9941	444	239	9
musk	0.971	1.0	1.0	1.0	1.0	2965	97	166
http	0.9892	0.9923	0.9996	0.9982	1.0	565287	2211	3
shuttle	0.9971	0.9899	0.9998	0.9953	1.0	45586	3511	9
satimage-2	0.9933	0.9982	0.9984	0.9984	0.9939	5732	71	36
WDBC	1.0	1.0	1.0	1.0	1.0	357	10	30
Average	0.8036	0.8265	0.8635	0.937	0.9457			

Table 1: Tabular comparison of our algorithm ($\nu = 50\%$) compared to our competitors. We also state the total number of normal and abnormal samples in this dataset and the number of features.